Chemical Engineering Journal 324 (2017) 194–202

Contents lists available at ScienceDirect

Chemical Engineering Journal

journal homepage: www.elsevier.com/locate/cej

Construction of full-color light-emitting N-based carbon nanodots and their efficient solid-state materials via tape-casting technology for warm WLED

Sai Lin, Mengyuan Chen, Ziwei Wang, Yijun Zhang, Rongrong Yuan, Xiaojuan Liang, Weidong Xiang *, Yongqiang Zhou *

College of Chemistry and Materials Engineering, Wenzhou University, Wenzhou 325035, China

HIGHLIGHTS

- The multicolor Cdots were synthesized by simple adjustment of reaction temperature.
- Solid-state materials were created by combination of organosilane and Cdots.
- Red Cdots films were tape-casted on the Ce: PiG substrate.
- The CF-PiG based WLED realizes a facile chromaticity tuning.

GRAPHICAL ABSTRACT

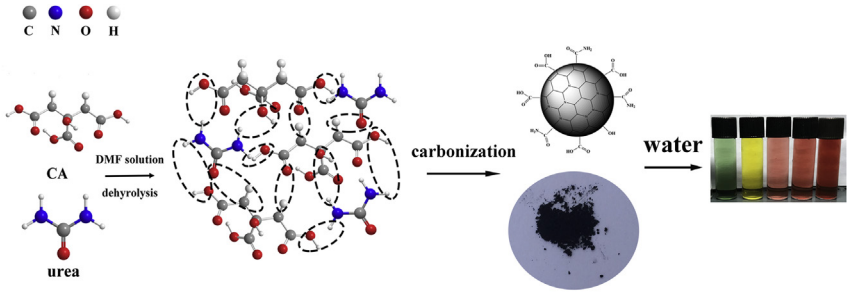

ARTICLE INFO

Article history:
Received 21 January 2017
Received in revised form 29 April 2017
Accepted 6 May 2017
Available online 8 May 2017

Keywords:
Multicolor Cdots
Solid-state materials
Tape-casting technology
Warm WLED

ABSTRACT

Multicolor luminescent carbon dots (Cdots) are of immense importance nowadays, while it still a challenge to construction of full-color light-emitting Cdots and their efficient solid-state materials. Here in, we fabricated a facile method to synthesize multicolor Cdots by adjustment of the reaction temperature. Although all samples showed uniform distribution of particles size and similar graphite structure, the surface chemical composition gradually varied among Cdots, especially the oxygen contents and nitrogen contents. Detailed material characterization has revealed that this tunable emission is results from the changes of the chemical composition. It is believed that the surface oxidation become more severe at high temperature, resulting in the formation of higher oxygen and nitrogen, which are responsible for the long-wavelength emission. Meanwhile, flexible solid-state materials were successfully created by combination of organosilane (OSi) and Cdots, which can be used to prevent the aggregation-induced solid-state fluorescence quenching. Finally, red Cdots/OSi was stacked on the $Y_3Al_5O_{12}:Ce^{3+}$ (Ce^{3+}: YAG) phosphor-in-glass (Ce-PiG) via tape-casting technology. Then, warm white light-emitting diodes (WLEDs) were constructed by these materials and GaN chips. As the Cdots increases, the correlated color temperature (CCT) decreases while the color rendering index (CRI) increases, and the color coordinates shift towards the red region. The resulting color converting material produced a warm white by adjusting red Cdots content, which will be a promising candidate for applications in the warm WLED.

* Corresponding authors.
E-mail address: xiangweidong001@126.com (W. Xiang).

http://dx.doi.org/10.1016/j.cej.2017.05.035
1385-8947/

1. Introduction

Due to the excellent quality in terms of luminescence, chemical stability, low toxicity, biocompatibility, carbon quantum dots (Cdots) have been attracting intensively attention over the past decade for potential applications in light-emitting diodes (LEDs), biomedical imaging, as well as sensor [1–5]. To date, various materials and hundreds of methods have been explored: top-down cutting and bottom-up carbonization routes are classified into two groups [6–8]. The former can effectively control the size, while the latter can effectively adjust the composition and physical properties of Cdots through using diversified carbon source and organic precursors [6,9]. Impressively, one key issue has been recognized is whether Cdots can be designed like quantum dots, so as to tune full color photoluminescence (PL), which is a crucial requirement successfully executing Cdots in the most application. Though many studies have synthesized emission-dependent excitation (EDE) Cdots, the PL wavelength still not cover the entire visible spectrum [6,10].

In fact, the common as-synthesized Cdots solution present blue to green luminescent, the highest reported that PL quantum yields (QY) of blue and green Cdots solution are more than 80%, 50% respectively [11]. In spite of a handful reports have reached red emission, the achievement of high QY long-wavelength Cdots solution is still a great challenge compared with short-wavelength Cdots. For instance, Pang et al. reported excitation-independent Cdots solution that centered at 608 nm and the QY only reached 1.8% [12]. Mandal and co-workers developed orange Cdots solution (centered at 590 nm, QY is 15%) [13]. A facile microwave for preparation of the pure red emissive Cdots solution is reported by Sun (centered at 640 nm) and the highest value of QY up to 22.9% [14]. Notably, most Cdots show strong PL in solutions, but CDs always undergo self-quenching in the solid-state, like organic molecules ascribed to excessive resonance energy transfer or direct π-π interactions [15], which greatly hinders their application [9,10]. Especially, color rendering index (CRI) exceed 80, correlated color temperature (CCT) under 4000 K, excellent spectral overlap with eye sensitivity functions and a warm white shade are required to design for an indoor light source [16]. For example, efficient red emissive Cdots in water (PL QY of 7%) have been reported by Bhunia [17], but the QY of powders was not mentioned. Qu et al. reported orange emissive Cdots solution, the PL quantum yield (QY) can up to 46% through surface Na^+ functionalization. However, the orange emissive Cdots are quenched in the solid aggregate states [11]. Chen and co-workers fabricated red Cdots PMMA film, similarly, they also evaded the PL QY of film [18]. Few work have been reported as far as we know on the preparation solid-state long-emission Cdots. Therefore, the development of solid-state red emissive Cdots will have a significant impact on the application of Cdots.

Herein, we reported a different approach by Qu [11] to shift PL peaks of Cdots from cyan to yellow and finally to red by controlling the reaction temperature. We demonstrated that higher temperature resulted in longer emission wavelength of Cdots. More important, solid-state Cdots films (CF) were successfully fabricated by incorporating the red Cdots into organosilane (OSi). The TeO_2-ZnO-Sb_2O_3-Al_2O_3-B_2O_3-Na_2O glass system was chosen as the optimal matrix for embedding Ce^{3+}: YAG phosphor and the tape-casting technique was used in the LED packages due to the controlled width, thickness and its compatibility with industrial processes. Using this technology, a homogeneous film using OSi blended with Cdots can be stacked on a Ce^{3+}: YAG phosphor-in-glass (Ce: PiG) substrate. Finally, the warm WLEDs were fabricated combined GaN, CF and Ce: PiG to generate white light, whose chromaticity can be tuned by simply varying red Cdots concentration. Thus, the work affords new opportunities to apply them in warm WLEDs.

2. Experiments

2.1. Materials

Anhydrous citric acid (CA), N,N-dimethylformamide (DMF), urea, N-(β-aminoethyl)-γ-amin-o-propyl methyldimethoxy silane (OSi), sodium hydroxide were purchased from Aladdin Chemistry Co.Ltd (Shanghai, China). Deionized water was used without further refinement. All of the chemicals used in the experiments were analytical grade and used as received without any further purification.

2.2. Synthesis of full-color light-emitting Cdots

Full-color light-emitting Cdots were synthesized by simple hydrothermal methods. In detail, 2 g CA (worked as C source) and 4 g urea (worked as N source) were dissolved in 20 mL DMF. Then the transparent solution was transferred into 40 mL Teflon-lined stainless autoclave. Next, the mixture placed on the oven and heated at different reaction temperature (120 °C, 140 °C, 160 °C, 180 °C and 200 °C) for 6 h. The samples were labeled as C-120, C-140, C-160, C-180 and C-200 respectively.

2.3. Fabrication of red-emission carbon nanodots solid-state materials

20 g OSi were added into 100 mL three-neck flask and heated at 240 °C under the nitrogen atmosphere and then cooled to room temperature. After that, the C-160/OSi solution was prepared by mixing Cdots (0.01–0.03 g) with 4 g OSi. Red emissive CF was obtained by depositing on the quartz glass via tape-casting technology, and then baking the samples at 100 °C for 24 h. The samples were denoted as CF-0.01, CF-0.02 and CF-0.03.

2.4. Preparation of warm WLED

In this paper, Cdots served as red phosphors in warm white LEDs. The Cdots/OSi solution was prepared by mixing C-160 (0.01–0.03 g) with OSi (4 g). Next, the mixture was heated at 100 °C for 3 h into slurries. Then, tape-casting technology was carried out to obtain Cdots tapes on the Ce: PiG substrate (Fig. 1). Finally, the Ce: PiG substrates covered with tapes are put into the oven at 100 °C for 24 h.

2.5. Characterization

The structural analysis of the Cdots were carried out using X-ray diffraction (XRD, D8 Advance, Bruker, Germany) measurements with a nikel filtered CuKa radiation in the range of 15–85° (2theta). To realize the microstructure of Cdots and the distribution of particles size, transmission electron microscopy (TEM) and high-resolution TEM (HRTEM) images were obtained using FEI Tecnai F20 operating at 200 kV. To realize the surface functional chemical group, the Fourier transform infrared (FTIR) spectra were detected, in which each sample was ground with KBr powder and measured using a Bruke Equinox 55 FTIR spectrometer from 500 to 4000 cm^{-1}. To further realize the surface structures of the Cdots, X-ray photoelectron spectroscopy (XPS) analysis was collected using an Axi Ultra DLD spectrometer with monochromatic Al Ka as the excitation source. UV–vis was recorded with a UV-2450 spectrometer, in which the each sample was placed in cuvettes (1.0 cm path length). Fluorescence spectra and PL QY was acquired using a Horiba Jobin Yvon Fluromax-4P spectrophotometer equipped with absolute QY measurement apparatus. Time resolved PL lifetime measurements were performed using a time-correlated single-photon counting (TCSPC) lifetime spectroscopy system with

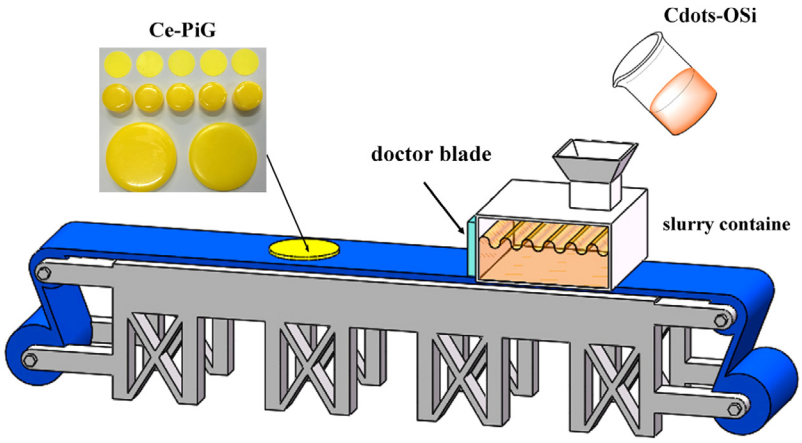

Fig. 1. The schematic of fabrication of CF stacked Ce: PiG plate.

a picosecond-pulsed diode laser (EPL-400 nm) as the single wavelength excitation light source. Optical properties such as color rendering index (CRI), color coordinates (CIE), correlated color temperature (CCT) and luminous efficacy (LE) were evaluated employing an integrating sphere (PMS-50, Everfine, China) under a forward current of 20 mA.

3. Result and discussion

The N-based Cdots were synthesized by directly dehydrolyzing, carbonizing starting materials CA and urea in the solution of DMF (Fig. 2). Interestingly, at different temperatures, we acquired a series of different color solution (the samples of C-120, C-140, C-160, C-180 and C-200 were cyan, yellow, red, red and red, respectively), as shown in Fig. 2. Meanwhile, multicolor Cdots films (CF) were easily fabricated via tape-casting technology (Fig. S1), which can effectively avoid fluorescence quenching of Cdots in solid-state.

3.1. Character and optical properties of Cdots

Fig. 3 shows the PL spectra of five samples and all the samples exhibit emission-dependent excitation (EDE) features. As depicted

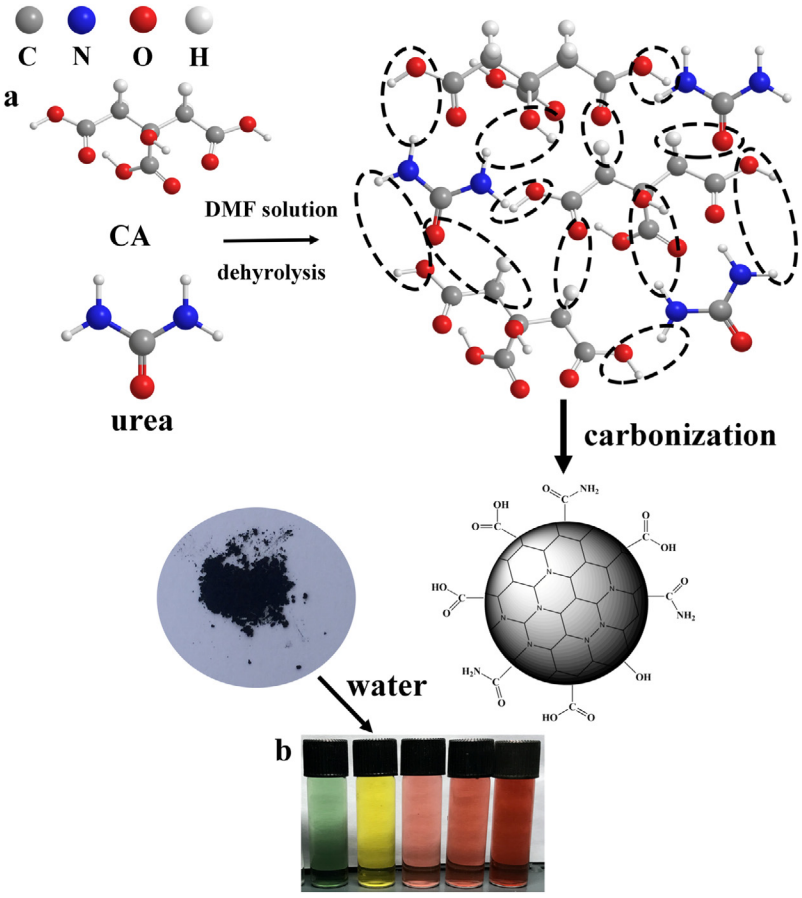

Fig. 2. (a) Growth process and the related structural model of N-based Cdots, (b) the picture of the Cdots dispersed in aqueous solution under sunlight (from left to right: C-120 to C-200).

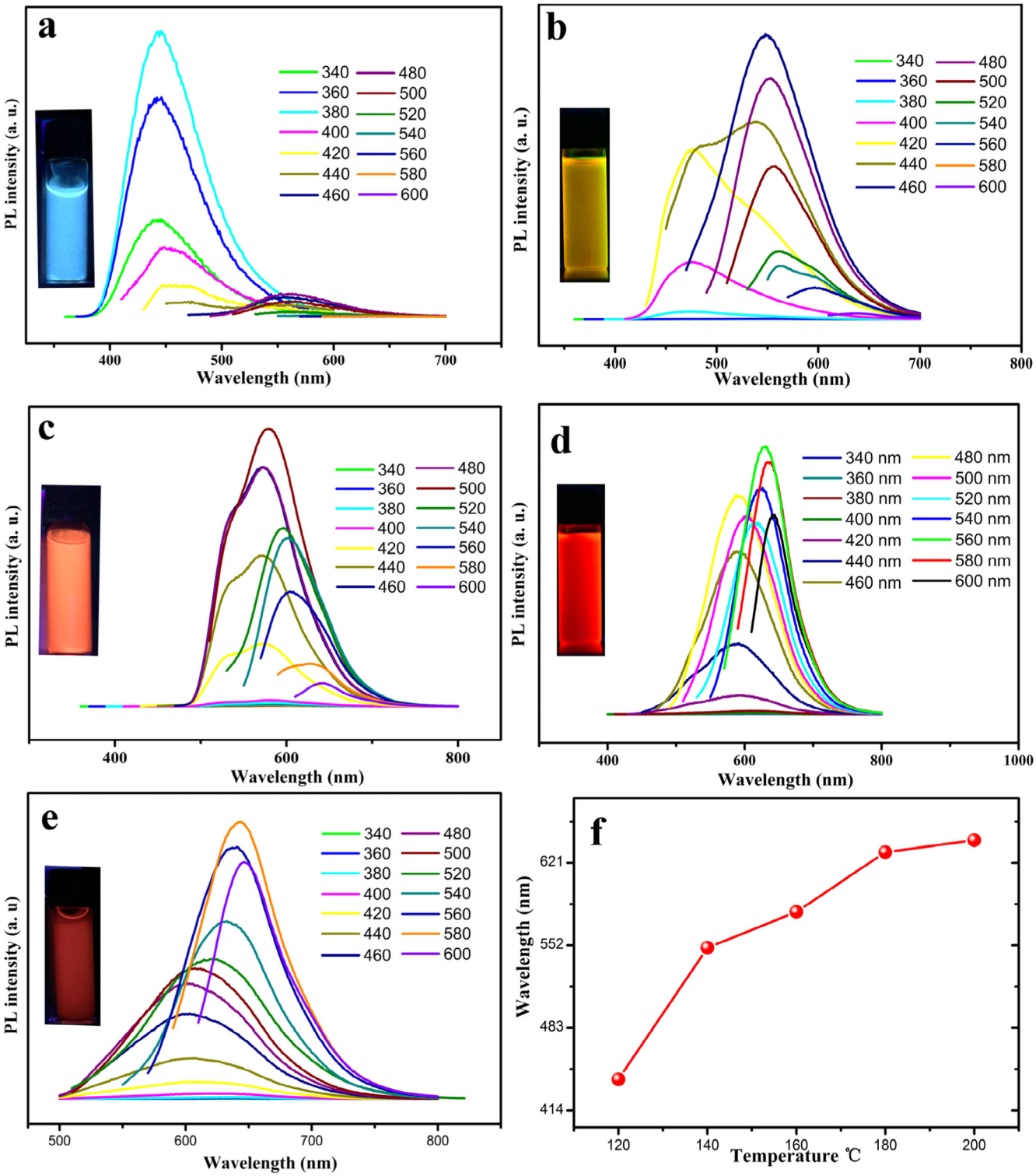

Fig. 3. (a-e) PL spectra of C-120 to C-200 under different excitation (recorded from 340 nm to 600 nm) and insets show the photographs of five samples taken under UV (365 nm) irradiation, (f) the PL emission peak under 460 nm irradiation.

in Fig. 3f, cyan, yellow, and red PL can be easily tune by increasing reaction temperature. Meanwhile, with the increasing of reaction time, the PL peak also shifted (Fig. S2). These obvious shifts, demonstrated that reaction temperature and reaction time do play a vital role in the tuning of PL peak. Interesting, in spite of this EDE features, C-120 and C-140 still cannot obtain long-wavelength emission. In contrast, the C-160, C-180 and C-200 can easy possess long-wavelength emission. It is worth nothing that the shifted peaks have much stronger PL intensity, which is quite different to the previously reported. What's the responsible for emission red shift? It may be that the surface oxidation become more severe at high temperature, resulting in the formation of more abundant organic functional groups, such as C═O, C═N [12,18–20]. It is believed that the surface states of Cdots are similar to a moecular

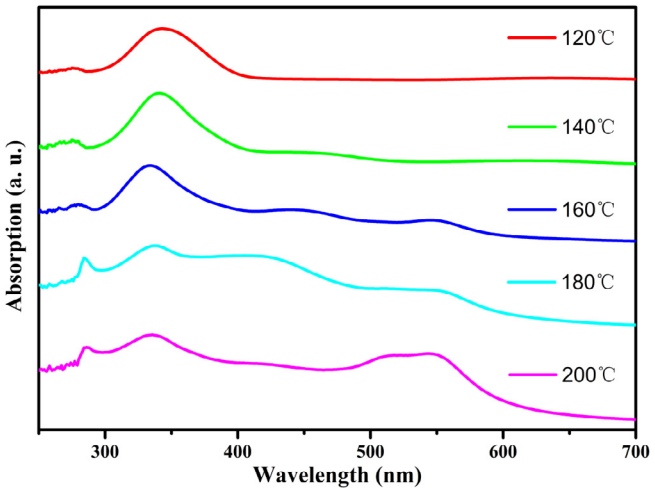

Fig. 4. The UV–vis spectra of Cdots.

state, wherein various surface states correspond to a relatively wide distribution of different energy levels, extending the excitation wavelength range and causing the EDE. The abundant surface functional groups, such as C═O and C═N, can efficiently introduce new energy levels for electron transitions and result in the continuously adjustable full color emissions [21], and meanwhile the possible energy level structures responsible for EDE was proposed, as schematically shown in Fig. S3 [19,20]. In addition, the quantum yields (QY) of Cdots in alkaline solution reached 45.6%, 48.5%, 46.2%, 29.6% and 28.7% respectively. Impressively, the QY of full-color light-emitting Cdots is quite high compared with others multicolor Cdots [12–14].

The UV–vis absorption spectra are depicted in Fig. 4, which revealed that the reaction temperature can affect the absorption properties. C-120 shows two strong absorption bands (centered at 284 nm and 333 nm), while a very weak absorption band in the region of 400–500 nm is detected for C-140. In addition, intense multi-state absorption including 284, 333, 421, 547 nm absorption bands are observed for C-160, C-180 and C-200. Importantly, the band at 547 nm is obviously increased from C-160 to C-200. These distinct absorption bands indicating that these Cdots possess different surface states, and because of this, these Cdots possess different PL property [22]. The typical absorption band in the region of 200–300 nm is attributed to the π-π* transition of C═C bonds, while the bands in the region of 300–500 nm and 500–600 nm are attributed to the C═O bonds and C═N bonds respectively [17]. Therefore, high temperature will induce more defect states on the surface of the Cdots. As a result, the red emission Cdots will occur at higher temperature.

TEM is used to characterize the morphology of the product. The dark spots in Fig. 5a correspond to the Cdots. It reveals that they are uniformly distributed and the size of Cdots is ranging from 2 nm to 4 nm (Fig. S4a). Furthermore, HRTEM image (inset of Fig. 5a) show clear-cut lattice fringes, which confirmed the crystalline feature of the as-synthesized Cdots. The lattice spacing is calculated as 0.241–0.243 nm, which is corresponds to the d-spacing of graphene {1−100} planes [11,23]. Interestingly, all samples are dispersed with similar average particles sizes (as shown in Fig. S5). The TEM dates clearly demonstrate that the quantum size effects are not the dominating element to cause the red-shift phenomenon [24]. Simultaneously, the AFM image

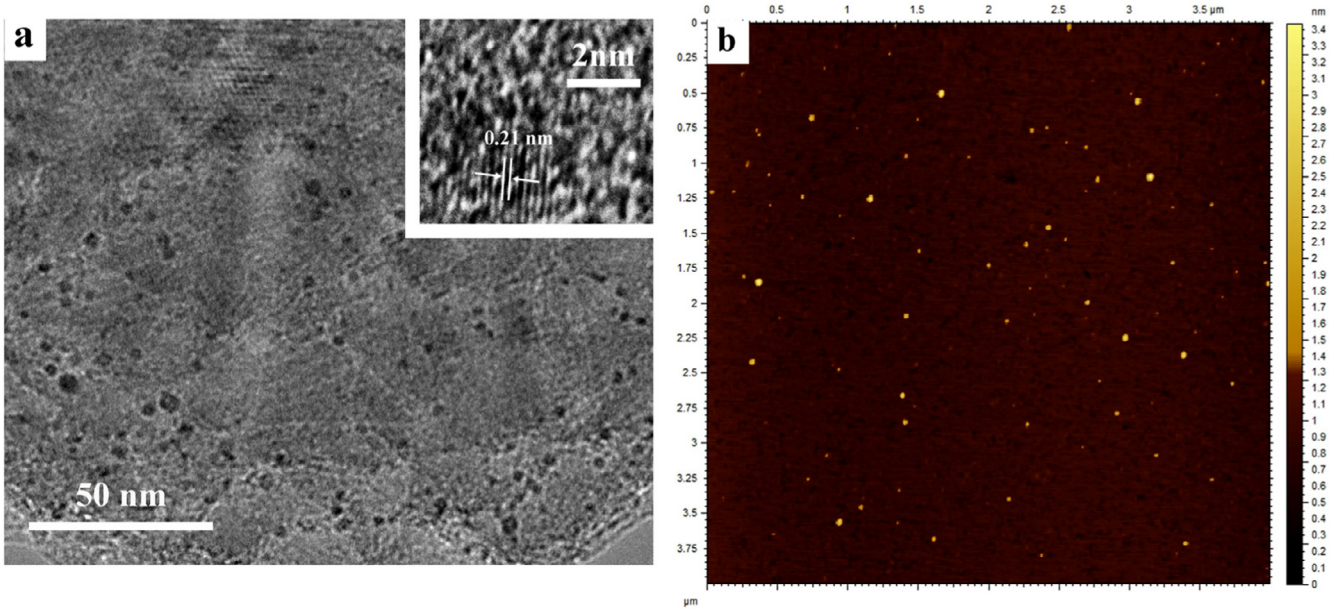

Fig. 5. (a) The typical TEM image of C-200. The inset in (a) is the HRTEM micrograph of an individual.C-200; (b) the AFM image of the C-200 deposited on freshly cleaved mica.

Table 1
XPS elemental analysis results of the C-160, C-180, C-200 samples.

Sample	C (mol%)	O (mol%)	N (mol%)	O/C (%)	N/C (%)
C-160	55.3	24.4	20.3	44.1	36.7
C-180	52.8	25.4	21.8	48.1	41.3
C-200	51.5	26	22.5	50.5	43.7

of Cdots indicates their heights was around to 3 nm, revealing that the Cdots possess eight to ten layers of graphene-like sheets [11]. The XRD pattern of Cdots is exhibited in Fig. S6, the broad peak at around $2\theta = 26°$ is attributed to (002) diffractions of graphitic carbon [25,26].

Knowing the surface functional groups of Cdots can help understand their luminescence mechanism. Therefore, XPS measurement is implemented to investigate the surfaces states of these Cdots. The Fig. S7 shows the full spectra of C-160, C-180 and C-200, which present three typical peaks: C 1s (~285 eV), N 1s (~400 eV) and O 1s (~532 eV) respectively. The strong N 1s peak reveals that the urea and DMF participates the reaction to synthesize the N-doped Cdots. Obviously, with an increase in reaction temperature, the nitrogen content and oxygen content gradually increase and the detailed dates are tabulated in Table 1. According to the reported by Hu, with O content increasing, a series of multi-state absorption are gradually increased, which is consisted with UV–vis [10]. Additionally, the emission of Cdots gradually red shifted as the result of higher temperature. In the high resolution spectra C 1s peak (Fig. 6a, d, g), the C 1s band has been mainly resolved into two peaks, representing graphitic sp^2 carbons (C=C/C—C, 284.5 eV) and carbonyl carbons (C=O 287.6 eV) [27]. The O 1s spectra (Fig. 6b, e, h) can be deconvuluted into two peaks located around at 531.7 eV and 533 eV, which are correspond to C=O and C—O respectively [28]. The spectra of N 1s are also measured and shown in Fig. 6c, f, i. The N 1s is fitted into two peaks at 399.7 eV and 401.8 eV, which are assigned to pyrrolic N and graphitic N [29]. The presence of graphitic N centers induces pronounced red-shift in the Cdots' absorption spectra, which is caused by an electron-doping effect that reduces the magnitude of the electronic gap [29].

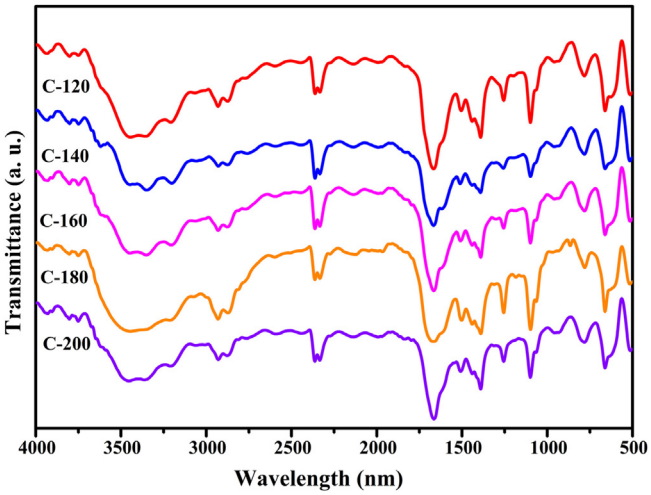

Fig. 7. The FTIR spectra of C-120, C-140, C-160, C-180 and C-200 (from top to bottom).

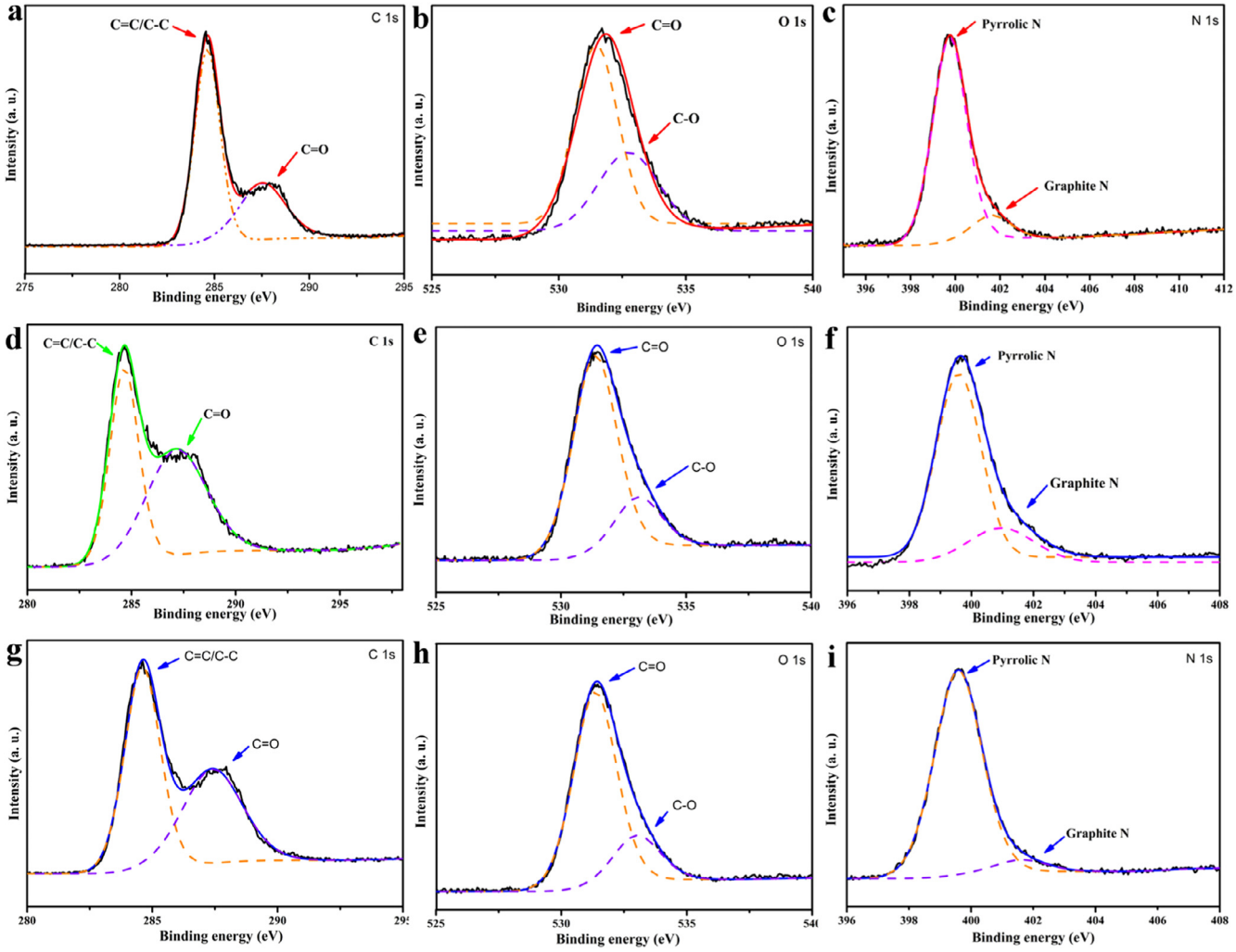

Fig. 6. The high resolution XPS spectra of (a,d,g) C 1s, (b, e, h) O 1s and (d, f, i) N 1s of C-160, C-180 and C-200 respectively.

As a supplement, FTIR spectra are characterized. As presented in Fig. 7, these five Cdots possess abundant hydrophilic groups, such as O—H (3450 cm^{-1}), N—H (3350 cm^{-1}), C—O (1388 cm^{-1}), which endow their excellent dispersibility in various solution (water, ethanol, DMF and so on). Meanwhile, stretching vibrations of C═O (1625 cm^{-1}) and C═N (1675 cm^{-1}), C—H_2 (1388 cm^{-1}) are observed, which is consisted with XPS results.

Although the PL mechanisms for Cdots remain vague, the amazing PL of Cdots continues to motivate researchers to conduct deeper explorations. Basing on UV–vis, TEM, AFM, FTIR, XPS dates, a series of results are summarized as follows: i) Short-wavelength luminescent Cdots more easily synthesized at low temperature while long-wavelength luminescent Cdots formed at high temperature. ii) High nitrogen contents and high oxygen contents are responsible for the long-wavelength emission.

3.2. Photoluminescence properties of Cdots films (CF)

Flurorescence is well-known to be often quenched when aqueous dispersion Cdots are drying. This shortcoming, explained by excessive resonance energy transfer or direct π-π interactions, significantly limits the wide applications. Hence, it is high time to establish effective method to preserve the PL abilities of Cdots in solid-state. In this paper, OSi is chose to as the precursor for a silica matrix for following reason. 1. OSi can be well compatible with Cdots because of abundant hydrophilic groups. Therefore, Cdots can be homogeneously dispersed in OSi to avoid aggregation, which overcomes poor dispersion of Cdots in traditional curing agent. 2. The two methoxy groups in OSi can be transformed into silanol groups after hydrolysis. 3. OSi neither competes for UV light with Cdots nor absorbs the emission of Cdots, the optical properties of Cdots can be unaffected after solidification. Therefore, Cdots embedded into OSi can be directly fabricated to form film through heat-treatment without other curing agent. Therefore, OSi can be directly established efficient red solid-state films and monoliths. Basing on the excellent property, the CF with different weight rate of C-160 are successfully fabricated.

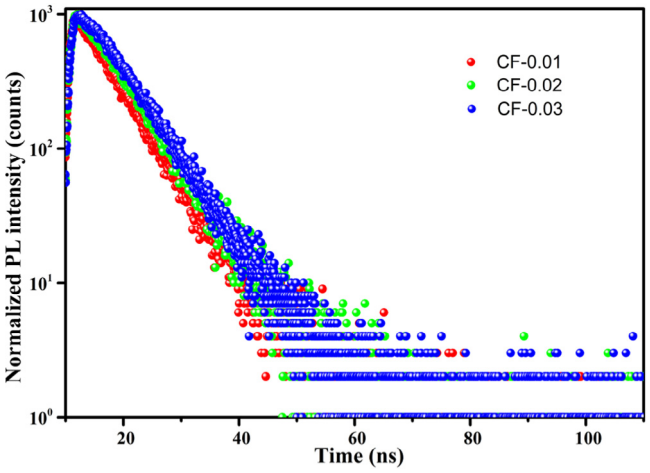

Fig. 9. The fluorescence lifetimes excited at 540 ns of CF-0.01, CF-0.02 and CF-0.03.

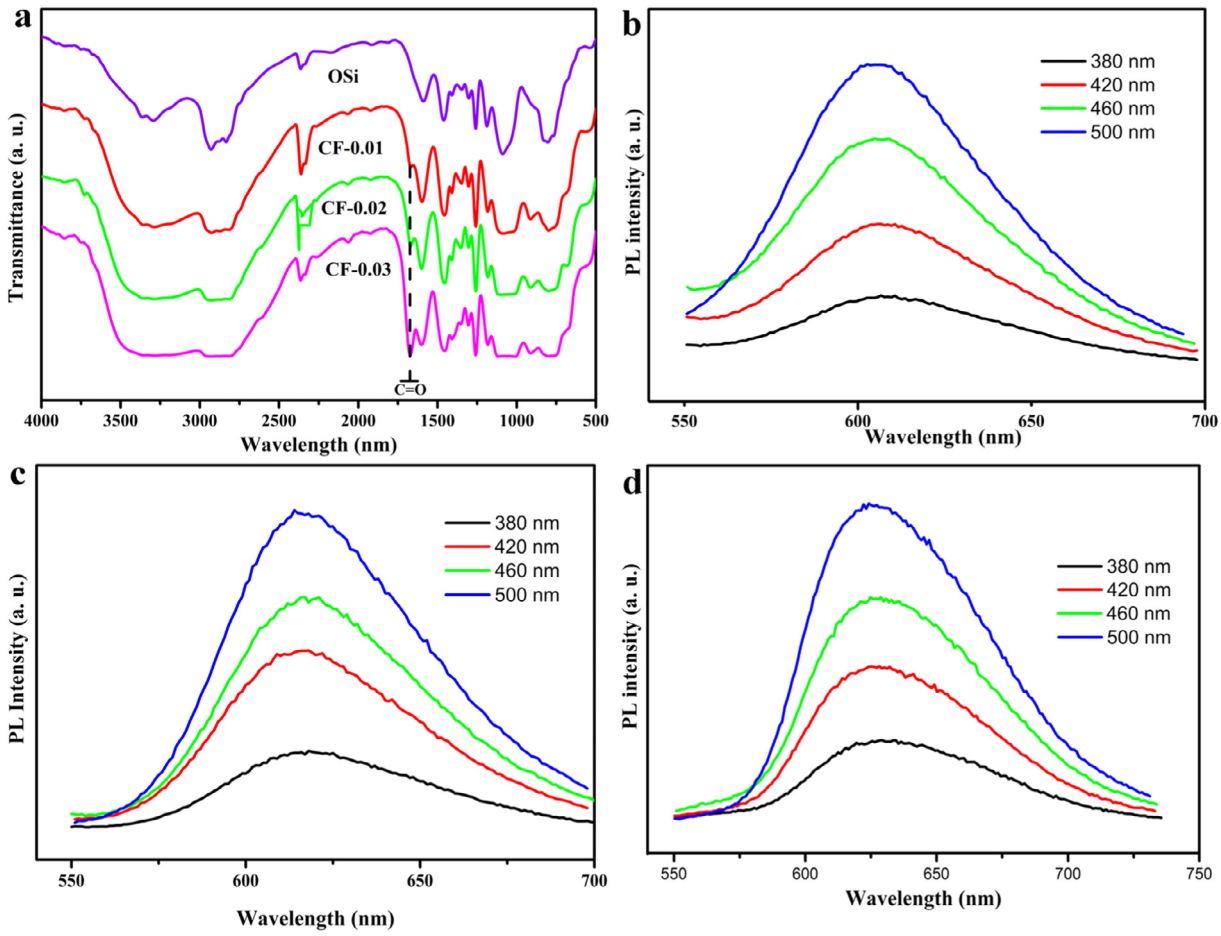

Fig. 8. (a) The FTIR spectra of OSi and CF; (b)-(d) the PL images of CF-0.01, CF-0.02 and CF-0.03 under the excitation wavelengths from 380 nm to 500 nm.

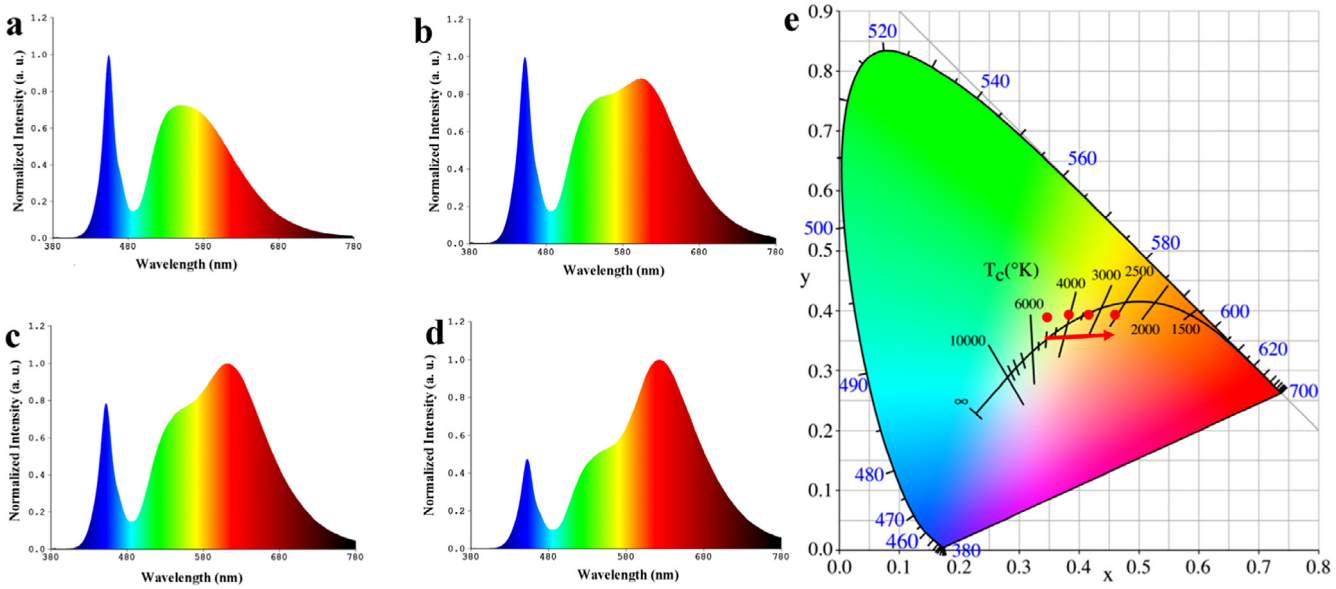

Fig. 10. (a)-(d) The normalized EL spectra for the fabricated the PiG-CF; (e) CIE color coordinates of the white LEDs fabricated by coupling the 460 nm blue light with PiG-CF.

Fig. 8a shows the OSi posses abundant hydrophilic group such as O—H (3450 cm^{-1}), N—H (1590 cm^{-1}), thereby vouchsafing the excellent water solubility of the OSi, and because of this, Cdots solution can be fully mixed with OSi. Different from the pure OSi, these samples CF-0.01 to 0.03 exhibit typical band that located at around 1635 cm^{-1}, which is ascribed to the C = ONR vibration. Fig. 8b-d show the PL spectra of the CF at several excitation wavelengths from 380 nm to 500 nm, and the PL emission peak clearly red-shifts with the increasing the Cdots contents. It can be attributed to the concentration of Cdots. For Cdots, the uniform dispersion in solvents at high concentrations could be unstable because of the extremely short distances between Cdots and high surface energy, which can cause dendritic aggregation. Such concentration-induced morphological changes finally caused red-shift.

Meanwhile, the thermal stability PL spectra of CF under the excitation at 460 nm in the range of 298 K to 438 K were characterized and shown in Fig. S8: the PL intensity decreased with increased temperature. It also exhibited no peak shift for CF. Compared with Cdots solution, the improved thermal quenching behavior of CF also demonstrates that solid-state CF is superior to Cdots solution in the potential applications.

The average lifetime of CF are determined using the TRPL technique. The TCSPC spectra excited at 540 nm of the CF with different doping weigh of Cdots are shown in Fig. 9. The fitted parameters are summarised in Table 2. The similar luminescent lifetime indicated the similar luminescent process [11]. Importantly, the CF QY is up to 19.2%, 22.2% and 25.8% respectively, further confirming that the CF, to some extent, can be used to overcome the fluorescence quenching when the Cdots are drying. In addition, different color solid-state materials can be easy acquired through adjusting Cdots and the above described solid-state composites can be easily mold-formed as different shapes, they may be attractive materials for various potential applications, including LED, biomedical imaging and even UV protection for optical devices.

Table 2
The PL lifetime and QY of the CF.

Sample	λ_{ex} (nm)	τ (ns)	QY (%)
CF-0.01	540	6.25	19.2
CF-0.02		6.51	22.2
CF-0.03		6.76	25.8

4. Application for warm WLED

Currently, the major commercial WLED, which contained GaN chip and yellow/green phosphor, suffers from high CCT and low CRI, owing to the lake of effective red component. To realize warm WLED, a Ce: PiG coated with CF (PiG-CF) was adopted as the color converter to construct a warm WLED. The TeO_2-ZnO-Sb_2O_3-Al_2O_3-B_2O_3-Na_2O glass system was chosen as the optimal glass matrix for embedding Ce^{3+}: YAG phosphor, as previously reported by our group [30]. The related PL and PL excitation (PLE) exhibit in Fig. 9S. As demonstrated in Fig. 10a-10d, the concentration-dependent electroluminescent (EL) spectra of the WLED, exhibit an emission band peaking at 460 nm from the GaN chip, a broad yellow emission from YAG and a red emission from CF. Obviously, the higher red Cdots content (as shown in Fig. 10a-d), the higher red component intensity and the weaker yellow intensity, which is due to to the absorption of blue light by the increasing of red Cdots.Content. As a result, the CCT of WLED decreases from 5037 K to 2561 K, while the CRI increases from 69.3 to 92.6. The related photoelectric parameters are listed in Table 3. The CIE

Table 3
Photoelectric parameters of warm WLEDs with different contents of C-160 under the operation current of 20 mA.

Samples	CCT (K)	CRI	LE (lm/W)	Chromaticity coordinates
PiG	5037	69.3	122.1	(0.3473,0.3895)
PiG-CF-0.01	4072	76.4	83.2	(0.3820,0.3930)
PiG-CF-0.02	3222	85.5	66.9	(0.4191,0.3917)
PiG-CF-0.03	2561	92.6	30.6	(0.4595,0.3925)

(Fig. 10e) of white LED shifts from cold white toward warm white with the increasing of Cdots contents. These results demonstrate that the color properties of light from WLED can be easily controlled by adjusting red Cdots content in the tape-casting technique and the PiG-CF can be a promising candidates for the solide-state indoor lighting applications.

5. Conclusion

In conclusion, multicolor Cdots were successfully synthesized via a simple method. By controlling reaction temperature, Cdots with different oxygen contents, nitrogen contents and different luminescent emitting could be observed. The PL QY of C-120 to C-200 in alkaline solution reached 45.6%, 48.5%, 46.2%, 29.6% and 28.7% respectively. In addition, the as-synthesized red Cdots were used to fabricate solid-states materials with OSi. The achieved QY of CF was as high as 25%. By tape-casting technology, a series of PiG-CF specimens for warm WLED were successfully fabricated. Impressively, PiG-CF encapsulated WLED exhibits a tunable chromaticity by simple adjusting the relative red Cdots content in a proper layer. Benefiting from effectively red luminescence, the Cdots were demonstrated to have potential applications in warm WLED.

Acknowledgements

The authors are thankful to National Nature Science Foundation of China (Nos. 51472183 and 51672192).

Appendix A. Supplementary data

Supplementary data associated with this article can be found, in the online version, at http://dx.doi.org/10.1016/j.cej.2017.05.035.

References

[1] S. Zhu, Q. Meng, L. Wang, J. Zhang, Y. Song, H. Jin, K. Zhang, H. Sun, H. Wang, B. Yang, Highly photoluminescent carbon dots for multicolor patterning, sensors, and bioimaging, Angew. Gew. Chem. Int. Ed. 52 (2013) 3953–3957.
[2] Y.P. Sun, B. Zhou, Y. Lin, W. Wang, K.A.S. Fernando, P. Pathak, M.J. Meziani, B.A. Harruff, X. Wang, P.G. Luo, H. Yang, M.E. Kose, B. Chen, L.M. Veca, S.Y. Xie, Quantum-sized carbon dots for bright and colorful photoluminescence, J. Am. Chem. Soc. 128 (2006) 7756–7757.
[3] W. Shi, Q. Wang, Y. Long, Z. Cheng, S. Chen, H. Zheng, Y. Huang, Carbon nanodots as peroxidase mimetics and their applications to glucose detection, Chem. Commun. 47 (2011) 6695–6697.
[4] K. Hola, Y. Zhang, Y. Wang, E.P. Giannelis, R. Zboril, A.L. Rogach, Carbon dots—emerging light emitters for bioimaging, cancer therapy and optoelectronics, Nano Today 9 (2014) 590–603.
[5] X. Li, Y. Liu, X. Song, H. Wang, H. Gu, H. Zeng, Intercrossed carbon nanorings with pure surface states as low-cost and environment-friendly phosphors for white-light-emitting diodes, Angew. Chem. 54 (2015) 1759–1764.
[6] H. Tetsuka, R. Asahi, A. Nagoya, K. Okamoto, I. Tajima, R. Ohta, A. Okamoto, Optically tunable amino-functionalized graphene quantum dots, Adv. Mater. 24 (2012) 5333–5338.
[7] S. Zhu, Y. Song, X. Zhao, J. Shao, J. Zhang, B. Yang, The photoluminescencemechanism in carbon dots (graphene quantum dots, carbon nanodots, andpolymer dots): current state and future perspective, Nano Res. 8 (2015) 355–381.
[8] Y. Zhang, Y. Wang, X. Feng, F. Zhang, Y. Yang, X. Liu, Effect of reaction temperature on structure and fluorescence properties of nitrogen-doped carbon dots, Appl. Surf. Sci. 387 (2016) 1236–1246.
[9] L. Tang, R. Ji, X. Li, G. Bai, C.P. Liu, J. Hao, J. Lin, H. Jiang, K.S. Teng, Z. Yang, S.P. Lau, Deep ultraviolet to near-infrared emission and photoresponse in layered N-doped graphene quantum dots, ACS Nano 8 (2014) 6312–6320.
[10] S. Hu, A. Trinchi, P. Atkin, I. Cole, Tunable photoluminescence across the entire visible spectrum from carbon dots excited by white light, Angew. Chem. 54 (2015) 2970–2974.
[11] S. Qu, D. Zhou, D. Li, W. Ji, P. Jing, D. Han, L. Liu, H. Zeng, D. Shen, Toward efficient orange emissive carbon nanodots through conjugated sp(2)-domain controlling and surface charges engineering, Adv. Mater. 28 (2016) 3516–3521.
[12] L. Bao, C. Liu, Z.L. Zhang, D.W. Pang, Photoluminescence-tunable carbon nanodots: surface-state energy-gap tuning, Adv. Mater. 27 (2015) 1663–1667.
[13] V. Gude, A. Das, T. Chatterjee, P.K. Mandal, Molecular origin of photoluminescence of carbon dots: aggregation induced orange-red emission, Phys. Chem. Chem. Phys. 18 (2016) 28274–28280.
[14] S. Sun, L. Zhang, K. Jiang, A. Wu, H. Lin, Toward high-efficient red emissive carbon dots: facile preparation, unique properties, and applications as multifunctional theranostic agents, Chem. Mater. 28 (2016) 8659–8668.
[15] S. Qu, X. Wang, Q. Lu, X. Liu, L. Wang, A biocompatible fluorescent ink based on water-soluble luminescent carbon nanodots, Angew. Chem. 124 (2012) 12381–12384.
[16] H. Zhu, C.C. Lin, W. Luo, S. Shu, Z. Liu, Y. Liu, J.E. Ma, Y. Cao, R.S. Liu, X. Chen, Highly efficient non-rare-earth red emitting phosphor for warm white light-emitting diodes, Nat. Commun. 5 (2014) 4312.
[17] S.K. Bhunia, A. Saha, A.R. Maity, S.C. Ray, N.R. Jana, Carbon nanoparticle-based fluorescent bioimaging probes, Sci. Rep.-UK 3 (2013) 1473.
[18] D. Chen, W.W. Wu, Y. Yuan, Y. Zhou, Z. Wan, P. Huang, Intense multi-state visible absorption and full-color luminescence of nitrogen-doped carbon quantum dots for blue-light-excitable solid-state-lighting, J. Mater. Chem. C 4 (2016) 9027–9035.
[19] Y.H. Yuan, Z.X. Liu, R.S. Li, H.Y. Zou, M. Lin, H. Liu, C.Z. Huang, Synthesis of nitrogen-doping carbon dots with different photoluminescence properties by controlling the surface states, Nanoscale 8 (2016) 294–297.
[20] X. Li, S. Zhang, S.A. Kulinich, Y. Liu, H. Zeng, Engineering surface states of carbon dots to achieve controllable luminescence for solid-luminescent composites and sensitive be2+ detection, Sci. Rep.-UK 4 (2014) 1–7.
[21] H. Nie, M. Li, Q. Li, S. Liang, Y. Tan, L. Sheng, W. Shi, S.X.A. Zhang, Carbon dots with continuously tunable full-color emission and their application in ratiometric ph sensing, Chem. Mater. 26 (2014) 6084.
[22] H. Ding, S.B. Yu, J.S. Wei, H.M. Xiong, Full-color light-emitting carbon dots with a surface-state-controlled luminescence mechanism, ACS Nano 10 (2015) 484–491.
[23] T.F. Yeh, C.Y. Teng, S.J. Chen, H. Teng, Nitrogen-doped graphene oxide quantum dots as photocatalysts for overall water-splitting under visible light illumination, Adv. Mater. 26 (2014) 3297–3303.
[24] B.B. Campos, M.M. Oliva, R. Contreras-Cáceres, E. Rodriguez-Castellón, J. Jiménez-Jiménez, J.C.G.E.D. Silva, M. Algarra, Carbon dots on based folic acid coated with pamam dendrimer as platform for pt(iv) detection, J. Colloid Interface Sci. 465 (2016) 165–173.
[25] Y. Yang, N. Liu, S. Qiao, R. Liu, H. Huang, Y. Liu, Silver modified carbon quantum dots for solvent-free selective oxidation of cyclohexane, New J. Chem. 39 (2015) 2815–2821.
[26] A. Barati, M. Shamsipur, H. Abdollahi, A misunderstanding about upconversion luminescence of carbon quantum dots, J. Iran. Chem. Soc. 12 (2015) 441–446.
[27] D. Qu, M. Zheng, L. Zhang, H. Zhao, Z. Xie, X. Jing, Z. Sun, Corrigendum: formation mechanism and optimization of highly luminescent n-doped graphene quantum dots, Sci. Rep.-UK 5 (2014) 7998.
[28] P. Zhang, C. Shao, Z. Zhang, M. Zhang, J. Mu, Z. Guo, Y. Liul, In situ assembly of well-dispersed Ag nanoparticles (agnps) on electrospun carbon nanofibers (cnfs) for catalytic reduction of 4-nitrophenol, Nanoscale 3 (2011) 3357–3363.
[29] S. Sarkar, M. Sudolská, M. Dubecký, C.J. Reckmeier, A.L. Rogach, R. Zbořil, M. Otyepka, Graphitic nitrogen doping in carbon dots causes red-shifted absorption, J. Phys. Chem. C 120 (2015) 1303–1308.
[30] J. Huang, X. Hu, J. Shen, D. Wu, C. Yin, W. Xiang, X. Liang, Facile synthesis of thermally stable Ce^{3+}: $Y_3Al_5O_{12}$ phosphor-in-glass for white LEDs, CrystEngComm 17 (2015) 7079–7085.